ISSN 2070-2051, Protection of Metals and Physical Chemistry of Surfaces, 2017, Vol. 53, No. 2, pp. 279–286. © Pleiades Publishing, Ltd., 2017.

NANOSCALE AND NANOSTRUCTURED MATERIALS AND COATINGS

The Effect of Nanoporous Silica Aerogel on Corrosion Protection Properties of Epoxy Coatings on Carbon Steel[1]

K. Akbarzade[a], M. R. Shishesaz[a], I. Danaee[a, *], and D. Zarei[b]

[a] *Abadan Faculty of Petroleum Engineering, Petroleum University of Technology, Abadan, Iran*

[b] *Technical Faculty, South Tehran Branch, Islamic Azad University, Tehran, Iran*

**e-mail: danaee@put.ac.ir*

Received December 12, 2015

Abstract—In this paper, due to special properties of aerogels such as ultra-low density and hydrophobic nature of aerogels, this nanomaterial was used as anticorrosive pigments. Silica aerogel was dispersed in epoxy resin by using sonication method. The dispersion of nanoparticles were characterized by transmission electron microscopy. The anticorrosive properties of these coatings were investigated by salt-spray and electrochemical impedance spectroscopy methods in a 3.5 wt % NaCl solution. Impedance parameters showed a decrease in coating resistance over immersion time. Results indicated that epoxy coatings containing nano silica aerogel could significantly increase the corrosion resistance of composite coatings compared to those of pure epoxy and the highest value was obtained for 0.5% aerogel nanocomposite coatings after 160 days immersion. Pull off adhesion test showed the highest value of adhesion was related to coating containing 0.5% aerogel. According to salt-spray methods, it was found that the best results were obtained with coatings containing 0.5 and 1 wt % of silica aerogel.

DOI: 10.1134/S2070205117020022

1. INTRODUCTION

Epoxies are widely used as the resin of different protective coatings since they show excellent adhesion, mechanical properties and chemical resistance in different media [1, 2]. However long exposures to wet and humid conditions attenuates barrier properties. Reinforcement of epoxy coatings by means of inorganic pigments was a common way to prolong the duration of protection [3–8].

Inorganic–organic composite materials are increasingly important due to their extraordinary properties, which arise from the synergism between the properties of the components [9–11]. Nanocomposites usually consist of nanosized mineral particles dispersed into a polymeric matrix. Silica, titania, carbon nanotubes and smectite clays have been widely applied for the reinforcement of polymeric materials [12–15]. The porous structure of aerogels is comparable to that of large pore mesostructures. Therefore, aerogels that have an open-pore structure can be readily adapted to polymer nanocomposites as reinforcing agents [16].

Silica aerogels are nanoporous materials with high specific surface area (500–1200 m^2/g), low density (0.003–0.1 g/cm^3), low dielectric constant (1.1–2.0) and low thermal conductivity (0.013–0.04 W/m K) [17]. These features have led the aerogels for various applications such as super thermal insulation, acoustic insulation, photoluminescent, radioluminescent and superhydrophobic aerogels for oil-spill cleanup [18–21]. Moreover, numerous studies have been published on application of silica aerogel in nanocomposites and many have focused on the use of aerogel in nanocomposite coatings [22–24]. But few studies have been published on aerogel/epoxy composites as follows. The hydrophobic and thermal insulation properties of silica aerogel/epoxy composite was studied by Ge et al. [17], and the effects of addition of aerogel nanoparticle on thermal insulation and hydrophobic properties of composite was discussed. By using transmission electron microscope, they proved that part of silica aerogels nanopores had been immersed by epoxy. Based on this phenomenon, an immersion model was build up to study the effect of immersion on the thermal insulation and hydrophobic properties. Kim et al. [22] investigated the effect of the silica aerogel for the mechanical reinforcement of thermoset epoxy polymers. They reported that the tensile modulus, tensile strength, elongation-at-break, and toughness of the nanocomposites were systematically enhanced in the presence of aerogel. Gupta and Ricci [25] investigated the effect of processing and compressive properties of aerogel/epoxy composites. They reported that the higher density composites lead to higher compressive modulus but lower yield strength.

[1] The article is published in the original.

Table 1. Physical properties of nanosilica aerogel

Property	Typical Values
Average pore diameter	~20 nm
Particle size	Micron to millimeters
Porosity	>95%
Average bulk density	0.06–0.08 g/cm^3
Tapping density	50–70 kg/m^3
Surface chemistry	Fully hydrophobic
Surface area	~680 m^2/g
Thermal conductivity	≤12 mW/m K

The aim of this work is to investigate the effect of nanoporous silica aerogel on corrosion protection of epoxy nanocomposite coatings. Firstly, silica aerogel nanocomposite coatings were prepared on steel plates. Nanoporous silica aerogel and fabricated nanocomposites were characterized by TEM techniques and the inhibition action of the silica aerogel nanoparticles was studied by salt spray and electrochemical impedance spectroscopy.

2. EXPERIMENTAL

2.1. Materials

Epoxy resin (Epon 828), with low viscosity made from bisphenol A and epichlorohydrin, and epoxy hardener F-206, a low viscosity modified cycloaliphatic amine curing agent, were purchased from Bajak Paint Company. Silica aerogel particles as additive material were purchased from Vakonesh Sanaat Part Company.

Table 1 provides an overview of the most important physical characteristics of silica aerogels. Cold rolled carbon steel panels with dimensions of 15 cm × 8 cm × 0.1 cm were used as metallic substrates. The steel substrates were abraded with sand papers of 120, 220, 320, 400 and 800 grades followed by toluene and acetone degreasing to remove any trace of surface oxides.

To prepare the silica aerogel/epoxy nanocomposites, a pre-determined amount of the silica aerogel was added to the epoxy resin (EPON 828) and mixed for 45 min by using a high shear impeller in a variable speed (900–1000 rpm) mixer. The resultant mixture was subjected to sonication for 45 min. The ultrasonication process was performed at a frequency of 20 kHz with an inlet ultrasound power of around 1 W/m L (UIP 1000 ultrasonic processor, Hielscher Ultrasound Technology). Subsequently, a stoichiometric amount of the hardener was then added with the mass ratio of the hardener to the epoxy resin set at 50/100 to the mixture and mixed. In order to reduce of air bubbles, the mixture was kept in vacuum chamber for 10 minutes. The coatings were applied on the steel sheets by means of an adjustable film applicator. The thickness of dry coatings was measured with Elcometer FN 4653 digital coating thickness meter (Elcometer Co. Ltd.) and showed that dry film thicknesses were obtained 30 ± 5 μm for all panels. To ensure the film curing, pre-curing of the nanocomposite was conducted in the laboratory atmosphere for a week before beginning the tests. At the end of preparation five formulations with 0, 0.25, 0.5, 1 and 2 wt % silica aerogel/epoxy resin nanocomposite coating were prepared.

2.2. TEM Analysis

The microstructure and the morphology of the silica aerogel was investigated using transmission electron microscope (TEM). The TEM specimens by using an ultra-microtome, OMU3 (Reichert, Austria), equipped with a diamond knife were cut from nanocomposite blocks. Thin specimens (70–100 nm) were cut from the cured film of the nanocomposite material of about 1 × 1 mm^2. The samples were placed on the 300 mesh copper grid. Transmission electron microscopy (TEM) images were obtained with a Philips-CM30 at an acceleration voltage of 150 kV.

2.3. Corrosion Tests

Electrochemical impedance spectroscopy (EIS) is known as a powerful and nondestructive useful technique in studying, measuring, and estimating coating resistance [26, 27]. The EIS measurements were performed at room temperature and the instrument used was an Autolab PGSTAT 302N Potentiosat/Galvanostat coupled with a FRA2 frequency response analyzer at open circuit potential. The measuring cell for EIS consisted of the coated sample panel as a working electrode of ~3.5 cm^2 in area, immersed in 3.5% NaCl solution, a platinum as the counter electrode and saturated calomel electrode (SCE) as a reference electrode. The measuring frequency was ranged from 100 kHz to 10 mHz with AC amplitude of 10 mV. The impedance diagrams were obtained at different exposure times up to 130 days.

Comprehensive salt spray test was performed to evaluate the corrosion resistance properties of the

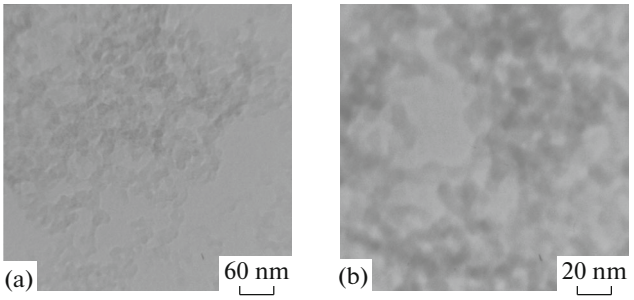

Fig. 1. TEM images of the nanosilica aerogel with different magnification.

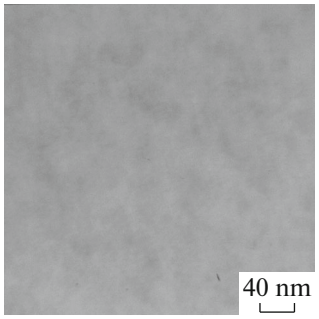

Fig. 2. TEM image of 0.5 wt % aerogel/epoxy resin nanocomposite coating.

coated mild steel plates according to ASTM B-117 method. A set of coatings with different formulations were applied on the steel sheets and the edge and backside of the substrates were covered by water-resistant tape. 5 wt % of sodium chloride solution was used for fogging. In order to observe the protective action of the coatings, the cross scribes were made down to the metal surface, then the steel panels were exposed to salt spray chamber (CTS-114D-B.AZMA co.) for 336 h.

2.4. Pull-off Adhesion Test

The pull-off adhesion tests were performed before and after salt spray test to measure the adhesion strength of the epoxy coatings with varying silica aerogel content. These tests were conducted using an Elcometer 106 Adhesion Tester with a maximum applied load of 20 MPa in accordance with ASTM D4541 type III. The dolly fixture with an area of 0.5 cm^2 was glued to the surface of the coated specimen using an appropriate adhesive (Cyanoacrylate MC1500). In the case of adhesion measurement after exposure, the samples were removed from the solution after 30 days immersion, rinsed completely with deionised water and allowed to dry for 48 h at ambient temperature. For each type of coating, measurements were done on three replicates and the average was taken.

3. RESULTS AND DISCUSSIONS

3.1. Microstructure of the Composites

Figure 1 shows that the TEM morphology of the silica aerogels have 3D nanoporous structure. The TEM micrograph of the silica aerogel pigment demonstrates that the diameters of nanopores are about 18–20 nm. The silica aerogel exhibits a sponge-like mesostructure. The brightness of particular areas in Fig. 1 shows the existence of pores in silica aerogel. After mixing aerogel in the resin, the composite retains the 3D net structure and part of the nanosized pores of the silica aerogels have been infiltrated by epoxy in Fig. 2. One of the applications of TEM analysis is to check whether the silica aerogel particles were evenly distributed in the epoxy resin matrix or otherwise. Due to the open pore structure and the hydrophobicity of the silica aerogels, these nanoparticles have been dispersed in the epoxy resin as shown in Fig. 2.

3.2. Electrochemical Impedance Spectroscopy Measurements

The Bode plot of the steel samples in the 3.5 wt % NaCl solutions without and with nano-silica aerogel pigments at different immersion times are shown in Fig. 3. The Nyquist plot of the steel samples immersed in 3.5 wt % NaCl solution after 160 days immersion are shown in Fig. 4. It is obvious that all Nyquist plots are in the form of semicircles. The semicircle diameter is an indicative of the coating resistance (R_c) against electrolyte diffusion. With increasing the concentration of silica aerogel up to 0.5 wt %, the semicircle diameter increases, however the addition of 1 and 2 wt % silica did not cause further increase in semicircle diameter.

With increasing immersion time up to 160 days, the coating impedance values decrease depending on water uptake content into the coating. By comparing the Bode plots, it can be seen that over a long period of immersion time, higher coating resistance is obtained in the presence of nanosilica aerogel. This means that nanosilica could significantly enhance the barrier properties of the epoxy coating by forcing the corrosive agents to travel a longer tortuous path to reach the substrate [13]. In addition, silica aerogel has hydrophobic nature which leads to decreasing water diffusion to epoxy coatings.

Table 2 shows the various electrochemical parameters for different exposure times. The electrical equivalent circuits used for numerical fitting of impedance plots at different exposure times are shown in Fig. 5 where R_s, R_c, and CPE_c represent solution resistance between the reference electrode and working electrode, coating resistance and constant phase element of coating capacitance. Constant phase element is often used instead of a capacitance to account for the non-ideal capacitive response from the interface [28]. A CPE is defined by the following equation:

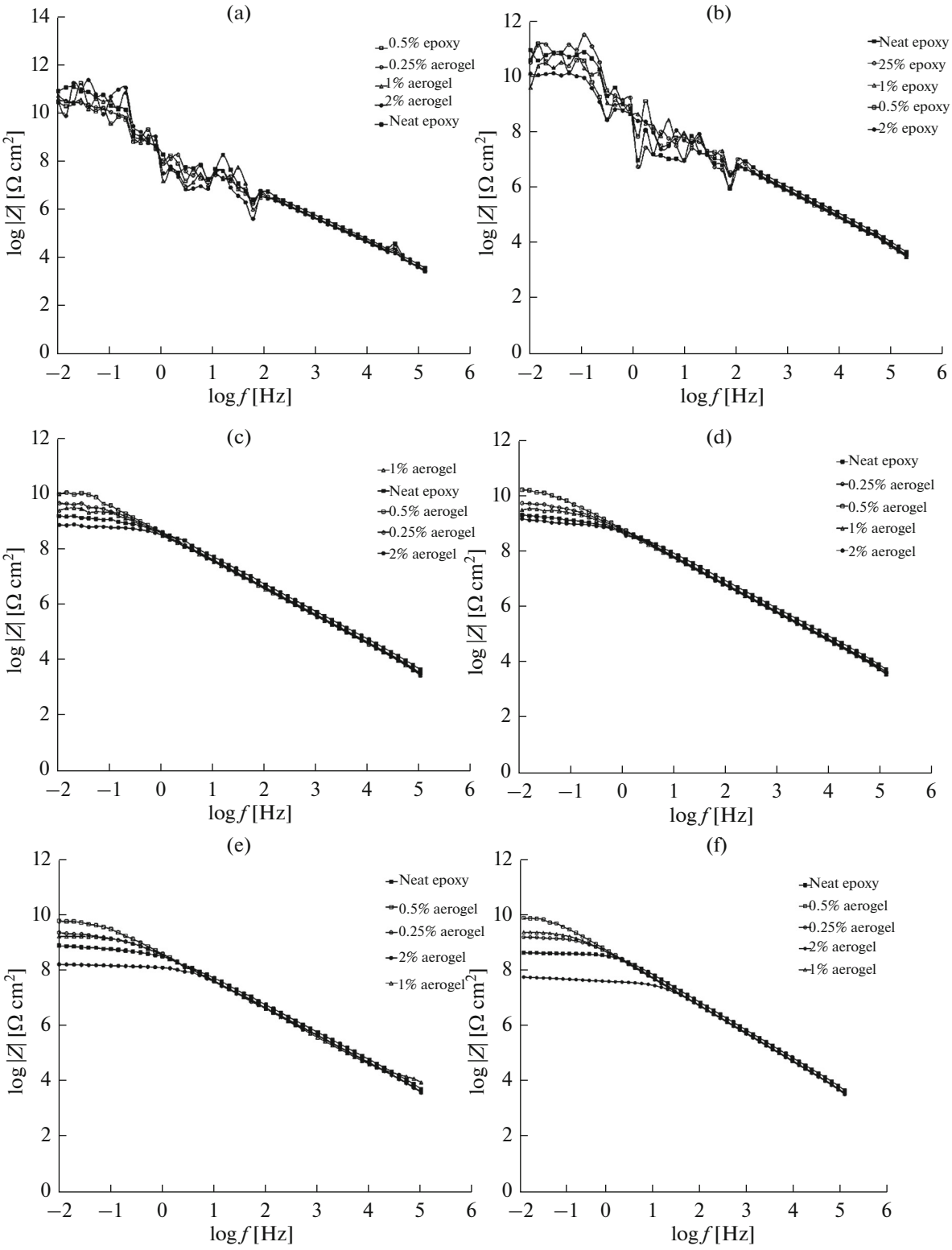

Fig. 3. Bode plot of the steel samples immersed in the 3.5 wt % NaCl solutions without and with nano-silica aerogel pigments at different times of immersion: (a) after 1 day immersion time, (b) after 30 days immersion time, (c) after 60 days immersion time, (d) after 90 days immersion time, (e) after 130 days immersion time, and (f) after 160 days immersion time.

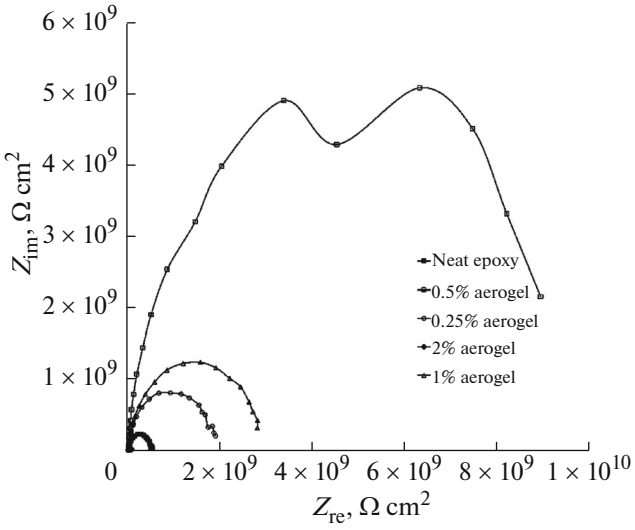

Fig. 4. Nyquist plot of the steel samples immersed in 3.5 wt % NaCl solution after 160 days immersion.

$$Z_{CPE} = \frac{1}{Y_0(j\omega)^n}$$

where Z is impedance of the CPE, ω is angular frequency ($\omega = 2\pi f$), n is CPE power, Y_0 is CPE constant which is a combination of properties related both to the surface and the electroactive species. The exponential factor n is often related to the degree of heterogeneity of the interface and/or surface film, i.e., the larger deviation from 1, the more heterogeneous surface layer [29]. According to Table 2, the R_c of the steel panels coated with epoxy resin and epoxy/aerogel nanocomposite coatings decreases as the immersion time increases. This indicates that the protective properties of the coating gradually decrease with increasing immersion times. However, in the presence of nanosilica in solution, R_c reduces with a lower rate. It can be seen that the higher R_c value is obtained for coating with 0.5 wt % silica aerogel. This indicates that up to 0.5 wt % silica aerogels nanopores is immersed by epoxy [17]. Due to the filling coating pores by some corrosion products, the decrease in R_c values is not regular and in some immersion time the value of R_c increases [30]. In the presence of higher amount of silica aerogel, the porosity of coating increases and therefore corrosion resistance decreases.

The capacitance values of all samples increases with increasing immersion. This can be attributed to water uptake which has a higher dielectric constant with respect to polymeric coating (the dielectric constant for water is at least four times greater than that of a typical organic coating.) and water diffusion can modify the dielectric constant of the polymer even if present in very small amounts [31]. It can be seen that the capacitance values of the coating containing 0.5 wt % nanosilica is less than the other samples. However,

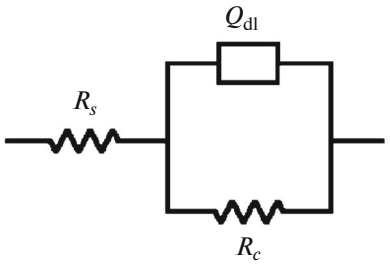

Fig. 5. Equivalent circuits used for fitting of the impedance plots obtained for the different immersion times.

due to the hydrophobic properties of aerogel water uptake rate is less than the neat epoxy. Variation of parameter n of the constant phase element with time (Table 2) shows that it decreases with the increase of immersion time. This can be attributed to increase in surface heterogeneity and coating degradation as a result of corrosive electrolyte diffusion into the coating matrix. According to Table 2, the CPE power values of the coating containing 0.5 wt % nanoparticles is higher than the other samples.

3.3. Salt Spray Test

The visual performances of the samples after salt spray test are shown in Fig. 6. As seen, after 336 h exposure, the blank epoxy coating is seriously corroded along the scribes. On the other hand, slight rust is observed on the coatings containing silica aerogel. These results show that addition of silica aerogel improves the corrosion protection performance of the coatings. Among the samples containing silica, it can be seen that the lowest rust is observed on the specimens containing 0.5 and 1 wt % silica. Moreover, it can be seen that the addition of nanoparticles to the epoxy coating decreases the delamination and water penetration around the scratches. Finally, no blister is created in all coated samples.

3.4. Adhesion Measurement

The dry and wet adhesions of coatings were measured and the results are presented in Table 3. It has been shown that the relationship between the dry adhesion and the corrosion resistance of an organic coating is not necessarily straightforward [32–34]. In addition, dry adhesion, compared to the wet adhesion, is not an appropriate parameter to predict anticorrosion properties of an organic coating [32, 33]. So, the wet adhesion, or the adhesion of a coating after exposure to moisture, water or a corrosive agent, is very important because in the presence of moisture, the conditions which occur in practical conditions, can be simulated and also there is a direct relationship between the adhesion of coatings and the coating resistance [35]. The dry and wet pull-off adhesion

Table 2. Electrochemical parameters extracted from EIS data for different immersion times

Sample		Immersion time							
		1 Day	16 Day	30 Day	45 Day	60 Day	90 day	130 day	160 day
Neat epoxy	R_c (Ω)	3.321×10^{11}	1.127×10^{10}	7.873×10^{10}	6.467×10^{9}	1.487×10^{9}	1.234×10^{9}	6.608×10^{8}	4.83×10^{8}
	Y_0 (F)	5.446×10^{-11}	1.061×10^{-10}	3.544×10^{-11}	1.983×10^{-10}	3.08×10^{-10}	3.403×10^{-10}	3.405×10^{-10}	2.886×10^{-10}
	n	1	1	1	1	0.9822	0.9725	0.9739	0.9911
0.25%	R_c (Ω)	4.639×10^{10}	3.424×10^{10}	2.297×10^{11}	2.574×10^{10}	4.877×10^{9}	3.714×10^{9}	2.056×10^{9}	1.788×10^{9}
	Y_0 (F)	1.651×10^{-10}	1.915×10^{-10}	1.052×10^{-11}	2.138×10^{-10}	4.175×10^{-10}	4.337×10^{-10}	4.445×10^{-10}	4.239×10^{-10}
	n	1	1	1	1	0.9832	0.9803	0.9778	0.9833
0.5%	R_c (Ω)	1.705×10^{11}	1.119×10^{11}	1.226×10^{11}	2.574×10^{10}	2.271×10^{10}	1.317×10^{10}	6.194×10^{9}	9.79×10^{9}
	Y_0 (F)	6.022×10^{-11}	1.121×10^{-10}	7.133×10^{-11}	2.138×10^{-10}	3.672×10^{-10}	3.95×10^{-10}	4.026×10^{-10}	$3.968\text{E} \times 10^{-10}$
	n	1	1	1	1	0.994	0.9863	0.9847	0.9854
1%	R_c (Ω)	9.603×10^{10}	2.066×10^{10}	2.589×10^{11}	1.928×10^{10}	3.119×10^{9}	3.841×10^{9}	1.715×10^{9}	2.695×10^{9}
	Y_0 (F)	1.601×10^{-11}	1.858×10^{-10}	6.87×10^{-12}	2.287×10^{-10}	4.465×10^{-10}	4.057×10^{-10}	4.717×10^{-10}	4.315×10^{-10}
	n	1	1	1	1	0.9853	0.9843	0.965	0.9792
2%	R_c (Ω)	3.115×10^{11}	9.229×10^{10}	1.087×10^{10}	1.722×10^{9}	5.471×10^{8}	4.535×10^{8}	1.145×10^{8}	5.478×10^{8}
	Y_0 (F)	2.238×10^{-11}	6.364×10^{-11}	2.68×10^{-10}	3.758×10^{-10}	4.725×10^{-10}	3.665×10^{-10}	3.642×10^{-10}	3.95×10^{-10}
	n	1	1	1	0.9875	0.9741	0.9803	0.992	0.9837

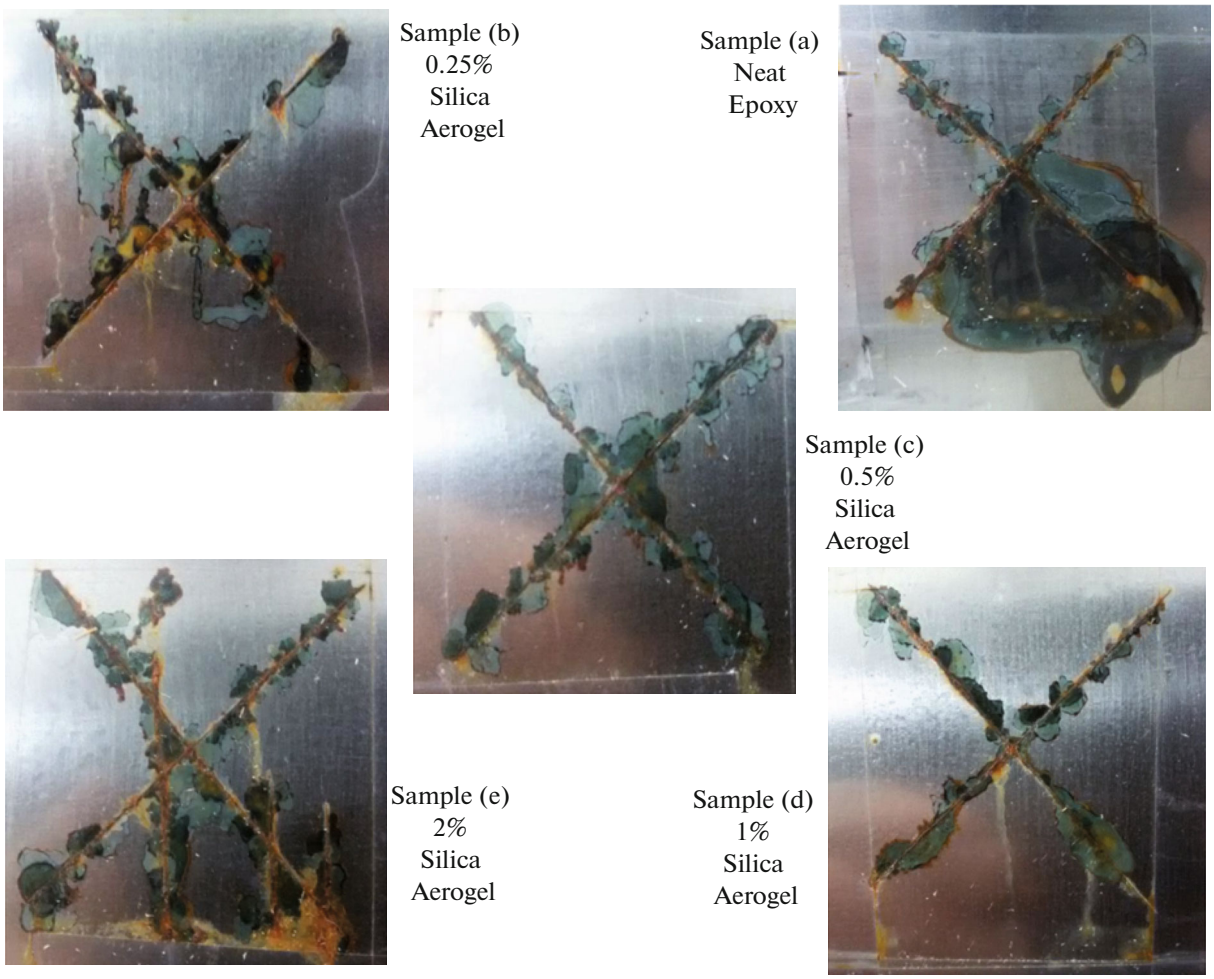

Fig. 6. Surface appearance of the samples after exposing to salt spray for 336 h.

strengths of the nanocomposites were measured after 30 days immersion. The results indicate that the wet adhesion strength of the coating containing different value of silica aerogel up to 1 wt % improves compared with the neat epoxy coatings. Coating containing 0.5 wt % of the nanoparticles has the highest adhesion to steel. Improving the adhesion of coatings may be attributed to the uniform dispersion of silica aerogel which leads to lower water and corrosive ions penetration and therefore lower disbonding.

4. CONCLUSIONS

In this study, silica aerogel was used as a pigment in the epoxy resin with average pore diameter of about 20 nm. Results obtained in this study are summarized below:

1. TEM analysis showed that the aerogel have compatibility with epoxy coating matrix. In addition, TEM analysis showed that the composite retains the 3D net structure and part of the nanosized pores of the silica aerogels have been infiltrated by epoxy.

Table 3. Dry and wet adhesion and percentage of adhesion reduction after 30 days of exposure to 5% NaCl

Nanoparticle content, wt %	Dry adhesion, N mm^{-2}	Wet adhesion, N mm^{-2}	Adhesion reduction, %
0	2.28	1.1	51.75
0.25	2.93	1.3	55.63
0.5	3.68	1.5	59.24
1	3.09	1.37	55.66
2	2.4	0.95	60.42

2. According to salt-spray and electrochemical measurements, addition of aerogel significantly improved the anticorrosive properties of epoxy coating. The best results were obtained by the addition of 0.5 wt % aerogel to epoxy coating.

3. The equivalent circuit elements showed that the coating contain 0.5 wt % silica aerogel in comparison with the other samples have highest value of coating resistance and lower capacitance.

4. According to the results of wet pull off test, the decrease in wet adhesion strength of the neat epoxy coating was severer than nanocomposites. Nanosilica aerogel can reduce adhesion loss of the coating.

REFERENCES

1. Kozlova, A.A., Kondrashov, E.K., Deev, I.S., and Shchegoleva, N.E., *Prot. Met. Phys. Chem. Surf.,* 2014, vol. 50, p. 903.
2. Dalinkevich, A.A., Gumargalieva, K.Z., Marakhovskii, S.S., and Aseev, A.V., *Prot. Met. Phys. Chem. Surf.,* 2015, vol. 51, p. 1176.
3. Lyakhovich, A.M., Shakov, A.A., Lyalina, N.V., and Elsukov, E.P., *Prot. Met. Phys. Chem. Surf.,* 2014, vol. 50, p. 883.
4. Omelchenko, O.D., Gribkova, O.L., Tameev, A.R., Novikov, S.V., and Vannikov, A.V., *Prot. Met. Phys. Chem. Surf.,* 2014, vol. 50, p. 613.
5. Chuppina, S.V. and Zhabrev, V.A., *Prot. Met. Phys. Chem. Surf.,* 2013, vol. 49, p. 344.
6. Buyuksagis, A., Kara, S., and Aksut, A.A., *Prot. Met. Phys. Chem. Surf.,* 2015, vol. 51, p. 155.
7. Darmiani, E., Danaee, I., Rashed, G.R., and Zaarei, D., *J. Coat. Technol. Res.,* 2013, vol. 10, p. 493.
8. Danaee, I., Darmiani, E., Rashed, G.R., and Zaarei, D., *Iran. Polym. J.,* 2014, vol. 23, p. 891.
9. Loskutov, A.I., Uryupina, O.Ya., Grigor'ev, S.N., Kosheleva, N.V., Oshurko, V.B., Romash, E.V., Senchikhin, I.N., and Falin, A.V., *Prot. Met. Phys. Chem. Surf.,* 2015, vol. 51, p. 558.
10. Klimova, S.A., Inozemtseva, O.A., German, S.V., Gorin, D.A., Ilgach, D.M., Meleshko, T.K., and Yakimansky, A.V., *Prot. Met. Phys. Chem. Surf.,* 2015, vol. 51, p. 396.
11. Bahrami Panah, N., Payehghadr, M., Danaee, I., Nourkojouri, H., and Sharbatdaran, M., *Iran. Polym. J.,* 2012, vol. 21, p. 747.
12. El'tekova, N.A. and El'tekov, Yu.A., *Prot. Met. Phys. Chem. Surf.,* 2013, vol. 49, p. 261.
13. Zamanizadeh, H.R., Shishesaz, M.R., Danaee, I., and Zaarei, D., *Prog. Org. Coat.,* 2015, vol. 78, p. 256.
14. Darmiani, E., Rashed, G.R., Zaarei, D., and Danaee, I., *Polym.-Plast. Technol. Eng.,* 2013, vol. 52, p. 980.
15. Hamad, A. and Turaif, A., *Prog. Org. Coat.,* 2010, vol. 69, p. 241.
16. Guo, Y., Wang, H., and Zeng, L., *J. Non-Cryst. Solids,* 2015, vol. 428, p. 1.
17. Ge, D., Yang, L., Li, Y., and Zhao, J., *J. Non-Cryst. Solids,* 2009, vol. 355, p. 2610.
18. Ali, Z., Khan, A., and Ahmad, R., *Microporous Mesoporous Mater.,* 2013, vol. 203, p. 8.
19. Yalizay, B., Morova, Y., Dincer, K., Ozbakir, Y., Jonas, A., Erkey, C., Kiraz, A., and Akturk, S., *Opt. Mater.,* 2015, vol. 47, p. 478.
20. Xie, T., He, Y.L., Tong, Z.X., Yan, W.X., and Xie, X.Q., *Appl. Therm. Eng.,* 2015, vol. 87, p. 214.
21. Saboktakin, A. and Saboktakin, M.R., *Int. J. Biol. Macromol.,* 2015, vol. 72, p. 230.
22. Kim, N.H., Hwang, H.S., Lee, J.L., Choi, K.H., Park, I., *Proc.18th Int. Conference on Composite Materials,* Jeju Island, 2011.
23. Sanli, D. and Erkey, C., *J. Supercrit. Fluids,* 2015, vol. 105, p. 99.
24. Chęcmanowski, J.G. and Szczygieł, B., *J. Non-Cryst. Solids,* 2008, vol. 354, p. 1786.
25. Gupta, N. and Ricci, W., *J. Mater. Sci. Technol.,* 2008, vol. 198, p. 178.
26. Bahri, H., Danaee, I., and Rashed, G.R., *Surf. Coat. Technol.,* 2014, vol. 254, p. 305.
27. Kakaei, M.N., Danaee, I., and Zaarei, D., *Corros. Eng., Sci. Technol.,* 2013, vol. 48, p. 194.
28. RameshKumar, S., Danaee, I., RashvandAvei, M., and Vijayan, M., *J. Mol. Liq.,* 2015, vol. 212, p. 168.
29. Jamali, F., Danaee, I., and Zaarei, D., *Mater. Corros.,* 2015, vol. 66, p. 459.
30. Corfias, C., Pebere, N., and Lacabanne, C., *Corros. Sci.,* 1999, vol. 41, p. 1539.
31. Deforian, F., Fedrizzi, L., Rossi, S., and Bonora, P.L., *Electrochim. Acta,* 1999, vol. 44, p. 4243.
32. Bajat, J.B., Mišković-Stanković, V.B., Bibić, N., and Dražić, D.M., *Prog. Org. Coat.,* 2007, vol. 58, p. 323.
33. Bajat, J.B., Mišković-Stanković, V.B., Popić, J.P., and Dražić, D.M., *Prog. Org. Coat.,* 2008, vol. 63, p. 201.
34. Palraj, S., Selvaraj, M., and Jayakrishnan, P., *Prog. Org. Coat.,* 2005, vol. 54, p. 5.
35. Ramezanzadeh, B. and Attar, M.M., *Mater. Chem. Phys.,* 2011, vol. 130, p. 1208.